NASA Technical Memorandum 86763

NASA-TM-86763 19850025833

Prediction of the Flow-Field Interference Induced by the Long-Range Laser Velocimeter in the Ames 40- by 80-Foot and the 80- by 120-Foot Wind Tunnels

Michael S. Reinath and James C. Ross

August 1985

NASA
National Aeronautics and
Space Administration

NASA Technical Memorandum 86763

Prediction of the Flow-Field Interference Induced by the Long-Range Laser Velocimeter in the Ames 40- by 80-Foot and the 80- by 120-Foot Wind Tunnels

Michael S. Reinath
James C. Ross, Ames Research Center, Moffett Field, California

August 1985

National Aeronautics and
Space Administration

Ames Research Center
Moffett Field, California 94035

This Page Intentionally Left Blank

SYMBOLS

x	coordinate measured in free-stream flow direction
r	radial coordinate measured from LRLV longitudinal axis of rotation
v	normalized resultant velocity vector magnitude
α	velocity vector pitch angle
β	velocity vector yaw angle
θ	angle between r-direction and horizontal, measured counterclockwise and perpendicular to free-stream velocity

SUMMARY

The predicted flow disturbances induced in the test sections of the Ames 40- by 80-Foot and 80- by 120-Foot Wind Tunnels by the presence of the Long-Range Laser Velocimeter (LRLV) are presented. The predictions were made using a potential-flow paneling code to model the test section and the LRLV, and a calculation of the resulting flow field was made. The flow velocity and angularity were calculated at numerous locations in the flow field relative to the LRLV, and the results are presented.

INTRODUCTION

In practice, wind tunnel measurements of flow-field velocities are made using mechanical probes. Although widely accepted, this method is inherently intrusive; mechanical probes occupy a finite volume and, therefore, can have a significant influence on the flow. Also, the structure required for probe support may be large relative to the flow field of interest. This presents difficulties, especially when probe translation is required in order to survey a region of the flow. Remote, nonintrusive velocity measurements can be made, on the other hand, using a laser velocimeter (LV), and the need for mechanical probes as well as the support structure in the vicinity of the probe can thereby be eliminated.

Laser velocimeters have been successfully used to make detailed velocity measurements in small wind tunnel facilities through test section windows (ref. 1). Unfortunately, the use of test section windows for LV measurements is not practical in the large wind tunnels of the National Full-Scale Aerodynamics Complex (NFAC). In these tunnels, the measurement distances are too large for operation in the backscatter configuration. To overcome this difficulty, an LV has been developed that is designed to measure velocity from within the wind tunnel test section, as shown in figure 1. When this instrument is used, the measurement range can be held to within acceptable limits while preserving the ability to survey significant portions of the test section flow field. This device is designated the Long-Range Laser Velocimeter (LRLV) and is described in detail in references 2, 3, and 4.

Although the LRLV eliminates the need for mechanical probes and the associated support structure in the vicinity of the measurement location, the velocity measurements are not completely nonintrusive. The entire instrument is located in the test section flow field and hence will perturb the flow nearby. This study was undertaken to assess the magnitude of these perturbations.

POTENTIAL FLOW MODEL

A three-dimensional paneling code, VSAERO (refs. 5 and 6), is used to model the test section and the LRLV in order to estimate the flow-field disturbance induced by

the LRLV. The code is a surface-singularity panel method that uses quadrilateral panels upon which doublet and source singularities are distributed in a piecewise, constant manner. The code can simulate nonlinear effects (e.g., wake roll-up and boundary-layer effects); however, the calculations for this investigation were limited to potential flow with fixed-wake geometry.

A diagram of the LRLV is shown in figure 2. The paneled representation that was generated to model this configuration consists of 525 panels and is shown in figure 3. It should be noted that no attempt was made to accurately model the minor geometrical details (such as the overhang of the nose fairing and the tail cone, the exact nose shape, and the surface discontinuity at the window where the beams exit the LRLV) in this paneled representation. These details are not important in this study because only the far-field effects on the test section flow are of interest. The rail system, which attaches to the wind tunnel floor, as shown in figures 1 and 2, lies within the boundary layer of the floor and was also neglected. The LRLV height above the wind tunnel floor resulting from the presence of the rail system, however, was correctly modeled.

Figures 4(a) and (b) are two views of the paneled representation of the 80- by 120-Foot Wind Tunnel and the LRLV. This representation required 1,837 panels and clearly illustrates the small size of the LRLV in comparison to the 80- by 120-Foot Wind Tunnel test section.

A similarly paneled configuration was developed to represent the 40- by 80-Foot Wind Tunnel test section and the LRLV. This configuration, shown in figures 5(a) and (b), consists of 1,349 panels, and also clearly illustrates the relatively small size of the LRLV in comparison to this test section.

RESULTS AND DISCUSSION

To obtain an initial estimate of the flow disturbance induced by the LRLV, a flow-field calculation was made for a simple configuration in which the wind tunnel representations were omitted. In this configuration, the LRLV was represented as an extension from a reflection plane which simulated the presence of the ground. This is referred to in the remainder of the discussion as the free-air case. A second case was then formulated that consisted of the 40- by 80-Foot Wind Tunnel test section and LRLV representations, as depicted in figure 5, and is referred to as the 40-by-80 case. A comparison of the results of these two cases was made to determine whether significant additional information would be gained by proceeding with a third case consisting of the 80- by 120-foot test section and LRLV representations. Based on this comparison, it was concluded that the third case would not yield significant additional information.

The paneling code was used to calculate the flow velocities and angularities for both the free-air and 40-by-80 cases at specific points within the flow fields. The locations of these points form a series of six transverse planes (fig. 6) located at selected longitudinal positions relative to the LRLV. In each plane, the points are further organized to form a series of lines that extend radially from the cylindrical portion of the LRLV. The polar coordinate system used for position reference is shown in figure 6.

The plane at $x = 4$ ft is designated the LRLV Measurement Plane. This designation is made because its location was chosen to coincide with the plane in which LRLV velocity measurements are made. The interference induced in this plane is obviously of particular interest since it directly affects the accuracy of the LRLV velocity measurements.

The normalized resultant velocity in the Measurement Plane is presented in figure 7 for the free-air case, plotted versus radial distance, r, from the LRLV (fig. 6) for various values of θ. The corresponding pitch and yaw angles are shown in figures 8(a) and (b).

These data show clearly that the interference decreases rapidly with distance from the LRLV. An increase in resultant velocity in the range 1.1% to 1.7% occurs at about 5 ft from the LRLV, depending upon the value of θ. However, this value decreases rapidly to about 0.3% at 15 ft and to less than 0.1% at 35 ft, the respective measurement distances required to reach the 40- by 80-foot and 80- by 120-foot test section centerlines. Similarly, the induced pitch angle of about 0.9° at 5 ft decreases to about 0.06° at 15 ft and to 0.01° at 35 ft, while the induced yaw angle decreases from about 1.4° to 0.18° and to less than 0.01° at the same respective distances.

To illustrate how the values of velocity magnitude and angularity vary with longitudinal position relative to the LRLV, two sets of curves for the free-air case are presented in figure 9. Figure 9(a) shows the variation in velocity along lines extending vertically ($\theta = 90°$) from the LRLV at various values of x. Figure 9(b) is a similar plot for pitch angle. The curves show that the free-stream values are quickly approached as the distance, r, is increased. Large variations in either parameter are apparent only in close proximity to the LRLV. (Yaw angularity is not presented since this parameter is 0 for $\theta = 90°$.)

The normalized velocity predicted for the 40-by-80 case is presented in figure 10. Calculations were made to a distance of $r = 30$ ft, in this case, because the optics intended for use in the 40- by 80-Foot Wind Tunnel test section are not designed for use beyond this distance. The corresponding yaw and pitch angles are shown in figures 11(a) and (b). A comparison with the predictions presented for the free-air case is shown in figure 12 for $\theta = 90°$ and reveals the presence of only small differences. Specifically, smaller pitch and yaw angularities are predicted for the 40-by-80 case, accompanied by a slight increase in free-stream velocity resulting from blockage introduced by the LRLV. At $r = 10$ ft and $\theta = 0°$, for example, the pitch and yaw angle predictions are 0.04° and 0.12° less, respectively, than in the free-air case. These differences are largest close to the LRLV but decrease with r, since the angles for both cases converge to zero in the free stream. It should also be noted that the predicted interference induced by the LRLV in the 80- by 120-Foot Wind Tunnel must fall between the 40-by-80 and free-air cases, and that a conservative estimate of flow angle can be obtained by using the free-air values.

CONCLUDING REMARKS

A panel code was used for the prediction of the flow interference induced by the presence of the LRLV and results were obtained for two configurations: a case which consisted of the LRLV and a simple ground plane, and a case which consisted of

the LRLV and the 40- by 80-Foot Wind Tunnel test section. The predictions obtained show similar behavior for both cases, although smaller pitch and yaw angles were calculated for the case which consisted of the 40- by 80-Foot Wind Tunnel and the LRLV configurations. Taking the free-air case as a conservative estimate, maximum pitch and yaw angles of 0.06° and 0.18°, respectively, are predicted at a distance 15 ft from the LRLV, which is the minimum distance required to reach the 40- by 80-Foot Wind Tunnel test section centerline. An increase of 0.3% in velocity is also predicted at this distance. At the distance required to reach the 80- by 120-Foot Wind Tunnel test section centerline, the pitch and yaw angle predictions decrease to less than 0.01°, and the velocity to less than 0.1% of free stream.

Verification of these predictions is necessary in order to gain confidence in their accuracy, especially if they are to be used in correcting LRLV measurements. This verification is the subject of possible future work using the LRLV and applying the method described in references 3 and 4 for making three-dimensional velocity measurements. When this method is used it is possible to measure the velocity components at a particular point in the flow field from two different LRLV measurement ranges, and thereby provide the data required to determine the relative interference.

REFERENCES

1. Snyder, P. K.; Orloff, K. L.; and Aoyagi, K.: Performance and Analysis of a Three-Dimensional Nonorthogonal Laser Doppler Anemometer. NASA TM-81283, 1981.

2. Reinath, M. S.: Laser Velocimeter for Large Wind Tunnels. J. Aircraft, vol. 19, no. 12, Dec. 1982, p. 1100.

3. Reinath, M. S.; Orloff, K. L.; and Snyder, P. K.: A Laser Velocimeter System for the Ames 40- by 80-Foot Wind Tunnels. AIAA Paper 84-0414, Reno, Nevada, Jan. 1984.

4. Reinath, M. S.; Orloff, K. L.; and Snyder, P. K.: A Laser Velocimeter System for Large-Scale Aerodynamic Testing. NASA TM-84393, Jan. 1984.

5. Maskew, B.: A Computer Program for Calculating the Non-linear Characteristics of Arbitrary Configurations: Users Manual. NASA CR-166476, Dec. 1982.

6. Maskew, B.: Prediction of Subsonic Aerodynamic Characteristics: A Case for Low-Order Panel Methods. J. Aircraft, vol. 19, no. 2, Feb. 1982, pp. 157-163.

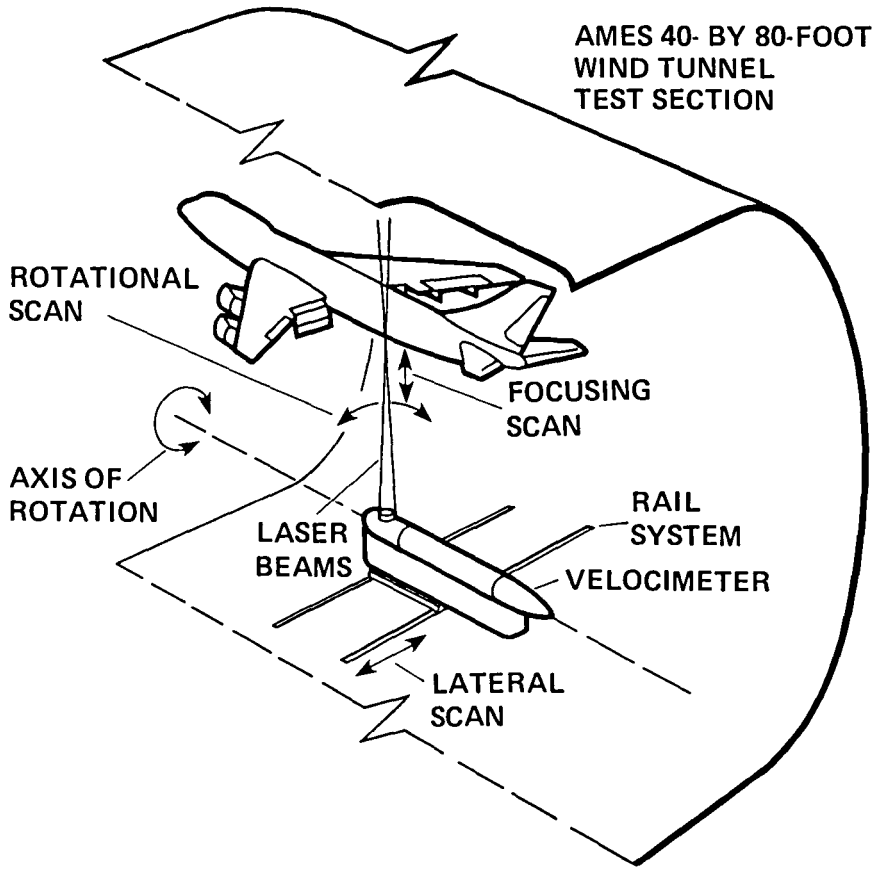

Figure 1.- Wind-tunnel application of the Long-Range Laser Velocimeter (LRLV).

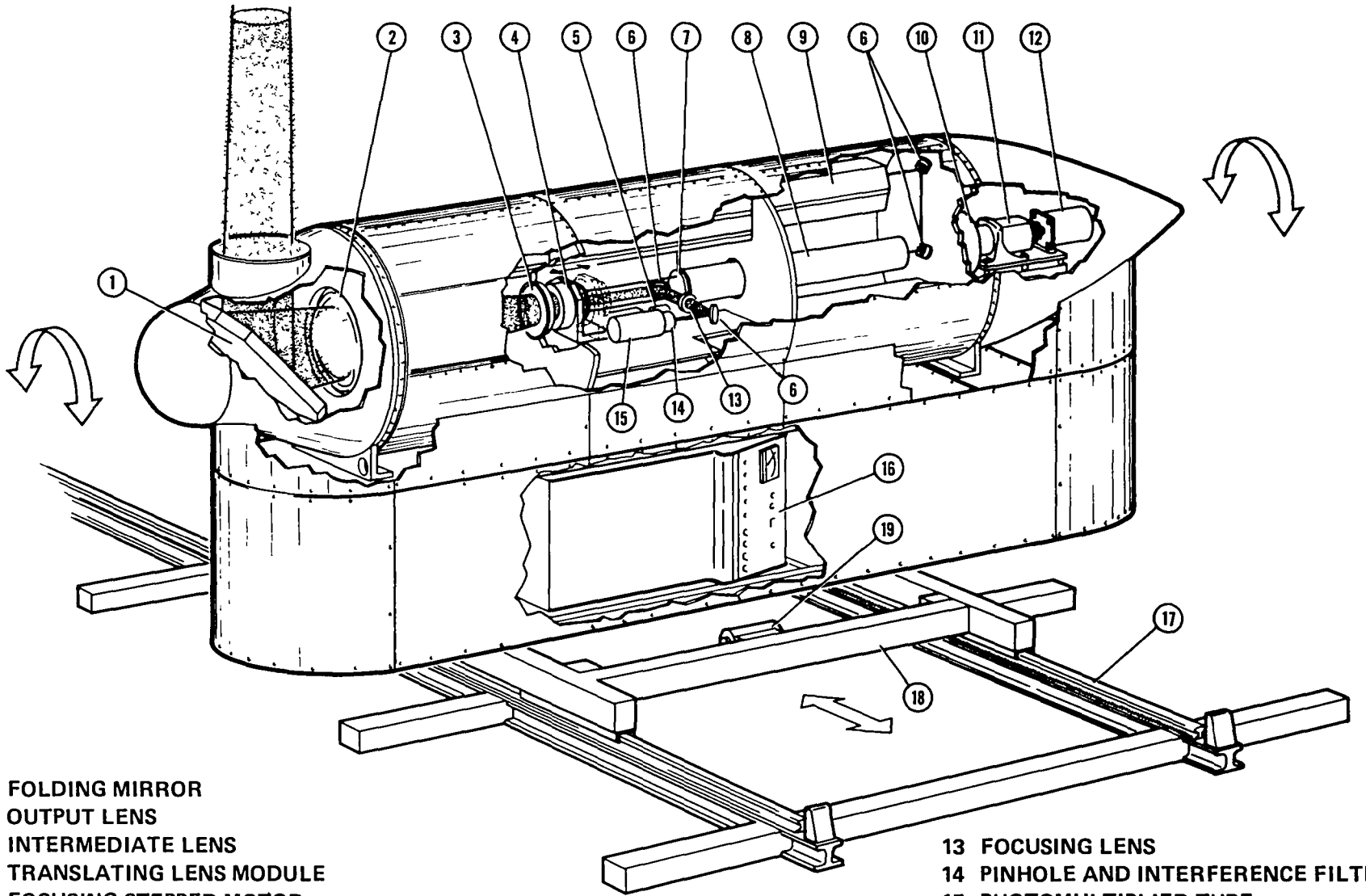

1 FOLDING MIRROR
2 OUTPUT LENS
3 INTERMEDIATE LENS
4 TRANSLATING LENS MODULE
5 FOCUSING STEPPER MOTOR
6 MIRROR
7 RHOMBOID ROTATOR ASSEMBLY
8 BEAM SPLITTER AND FREQUENCY SHIFTER
9 LASER
10 ABSOLUTE ENCODER
11 GEAR REDUCER
12 ANGLE ROTATION STEPPER MOTOR
13 FOCUSING LENS
14 PINHOLE AND INTERFERENCE FILTER
15 PHOTOMULTIPLIER TUBE
16 LASER POWER SUPPLY
17 LINEAR BEARING
18 TRANSLATION STAGE
19 LATERAL TRANSLATION STEPPER MOTOR

Figure 2.- The LRLV, drawn to scale, showing external fairings and also selected internal components.

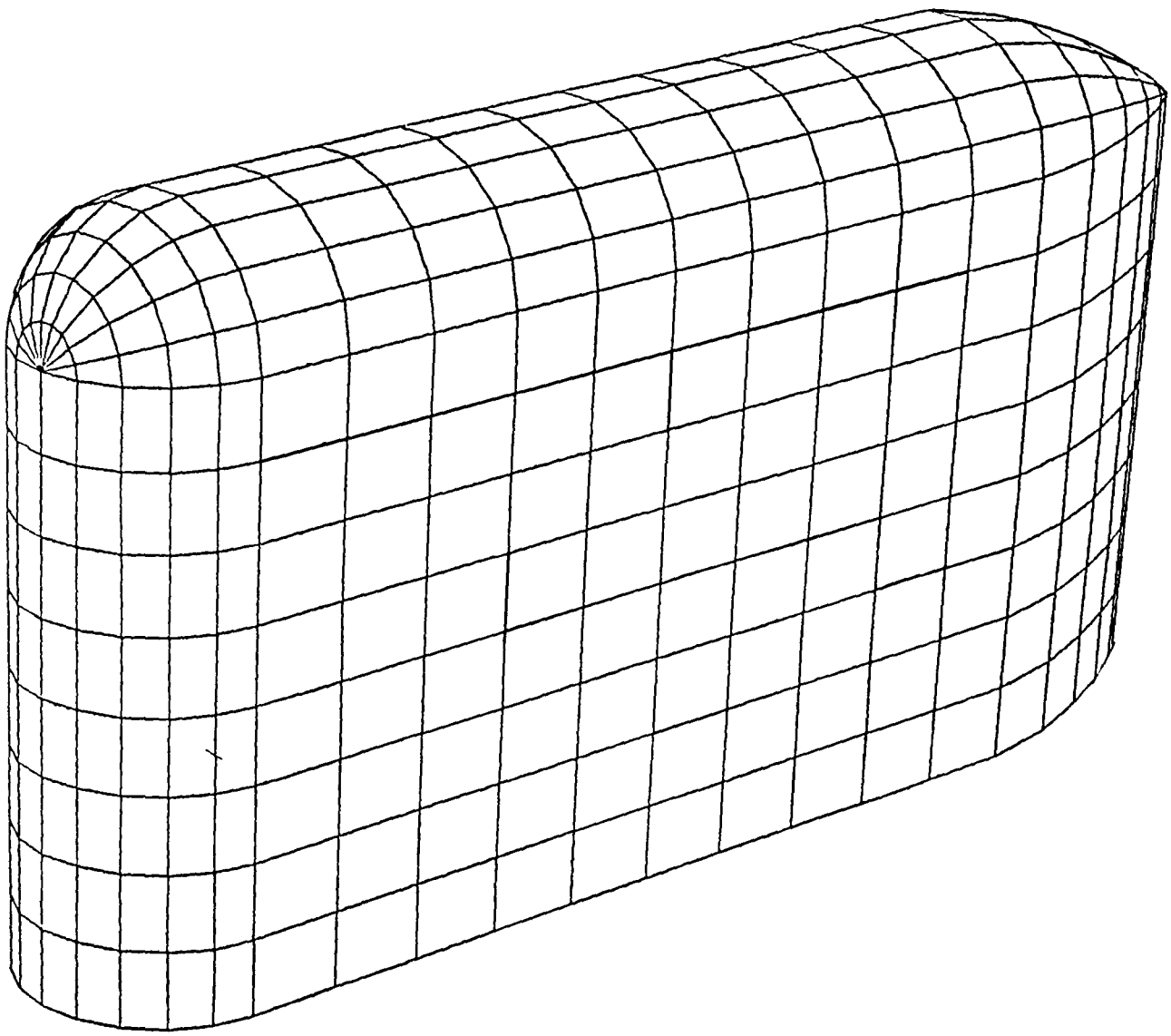

Figure 3.- Paneled LRLV representation.

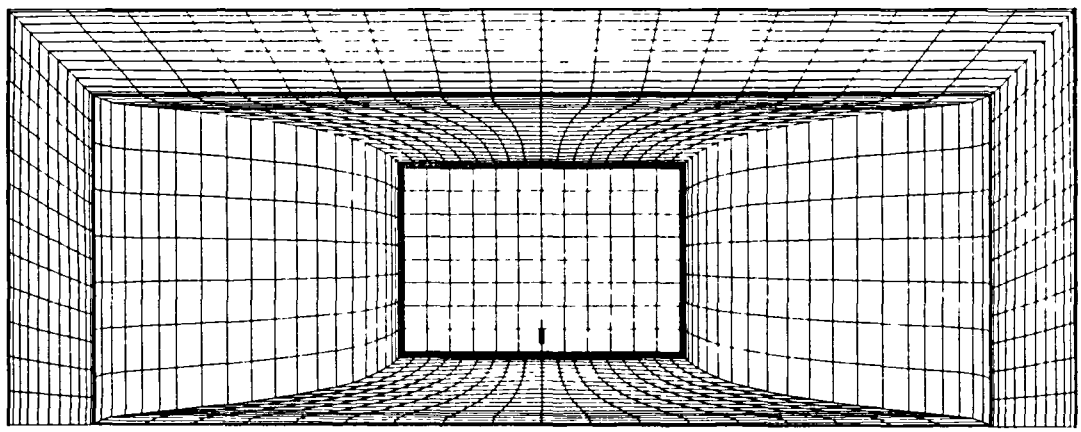

(a)

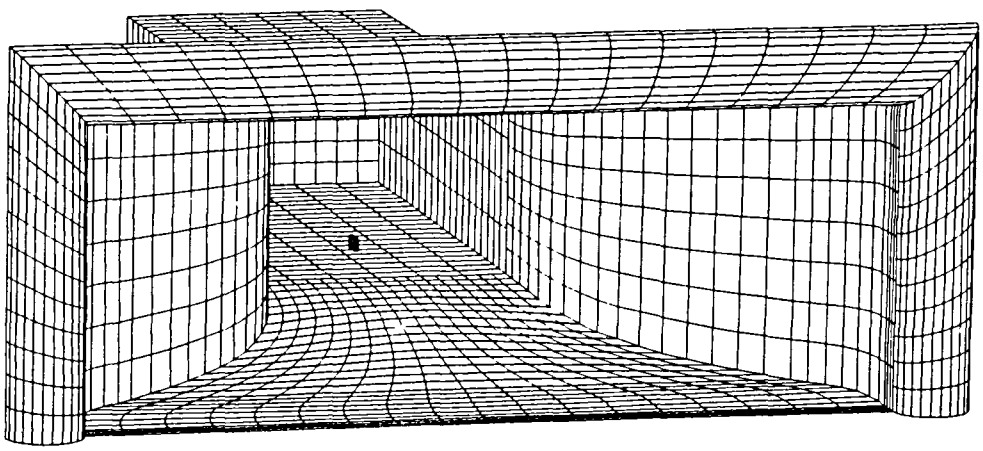

(b)

Figure 4.- The paneled representation of the 80- by 120-Foot Wind Tunnel showing the relative size of the LRLV from a viewpoint (a) on the inlet centerline, (b) above and to the left of the centerline.

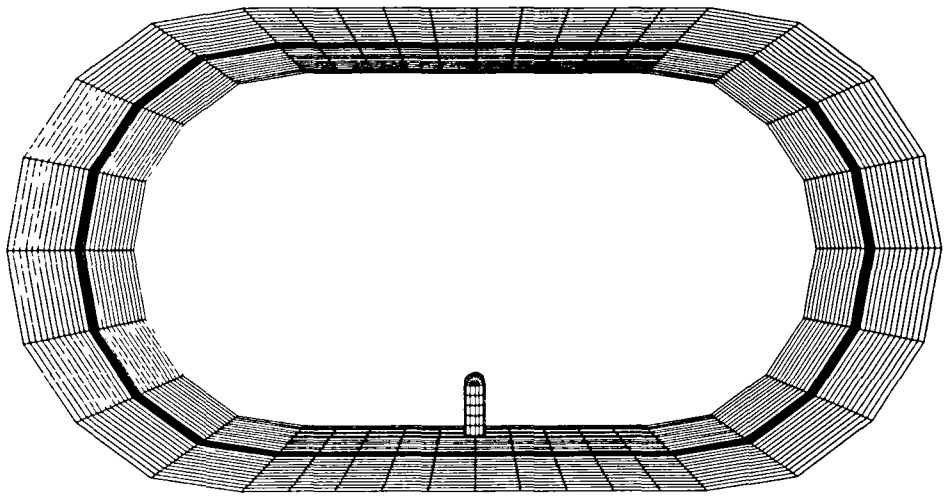

(a)

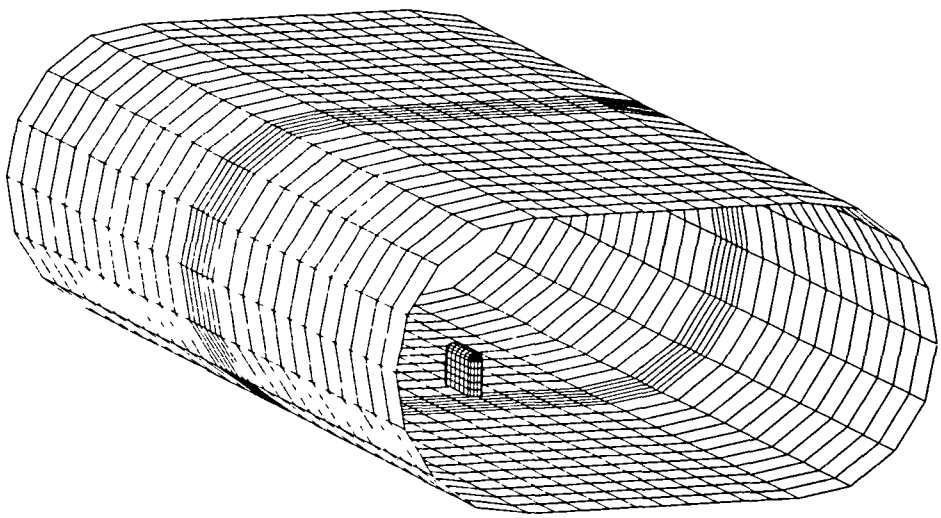

(b)

Figure 5.- The paneled representation of the 40- by 80-Foot Wind Tunnel test section showing the relative size of the LRLV from a viewpoint (a) on the test section axis of symmetry, (b) above and to the left of this axis.

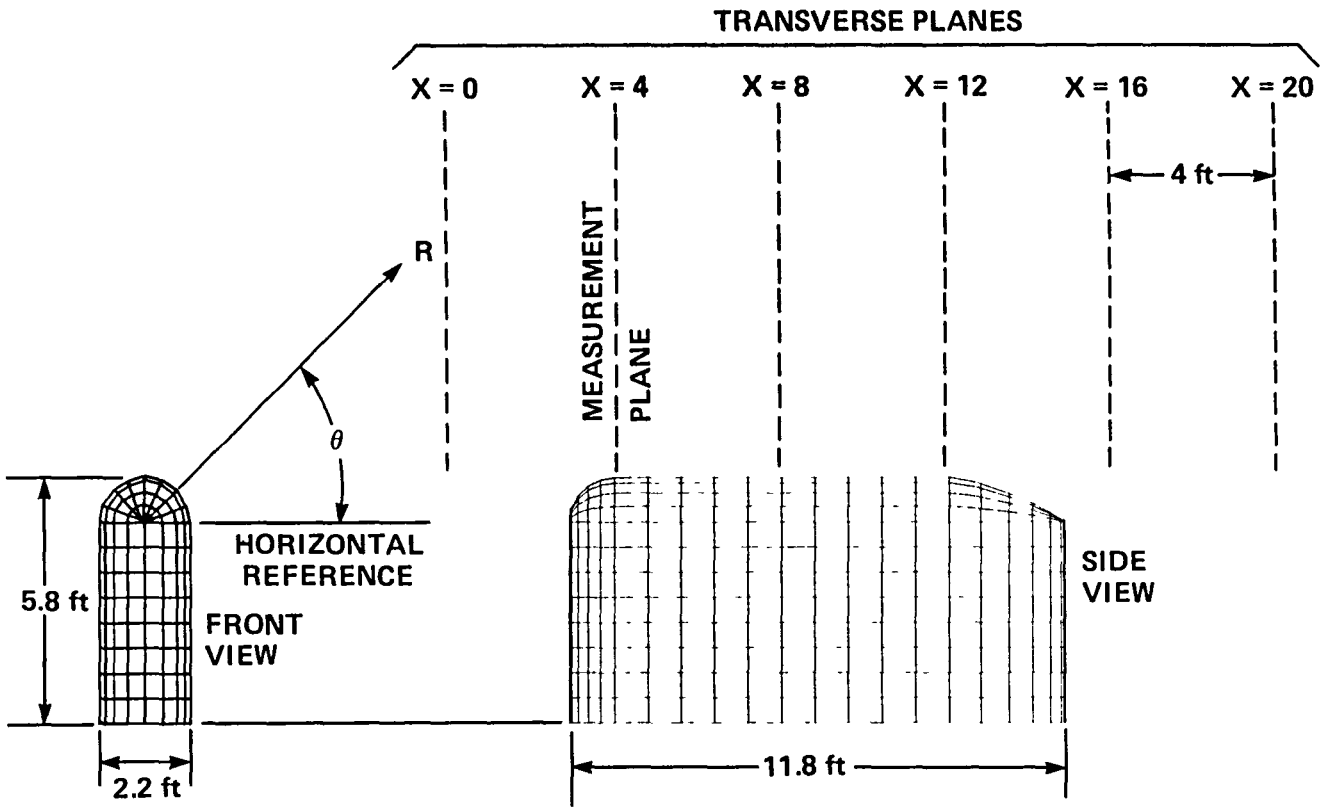

Figure 6.- The front and side views of the paneled LRLV representation showing the relative locations of the six transverse planes, the plane designated the Measurement Plane, and the polar coordinate system used to specify the locations of specific points within each plane.

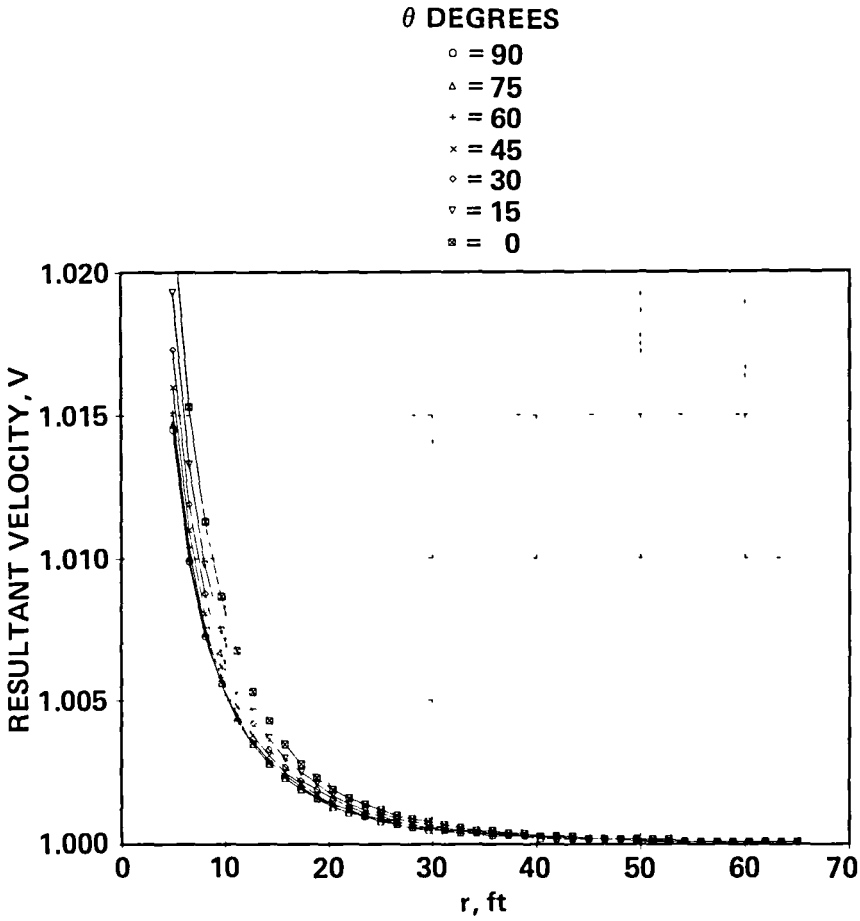

Figure 7.- Panel-code prediction of the normalized resultant velocity present in the Measurement Plane of the free-air case plotted versus radial distance, r, from the LRLV for various values of theta.

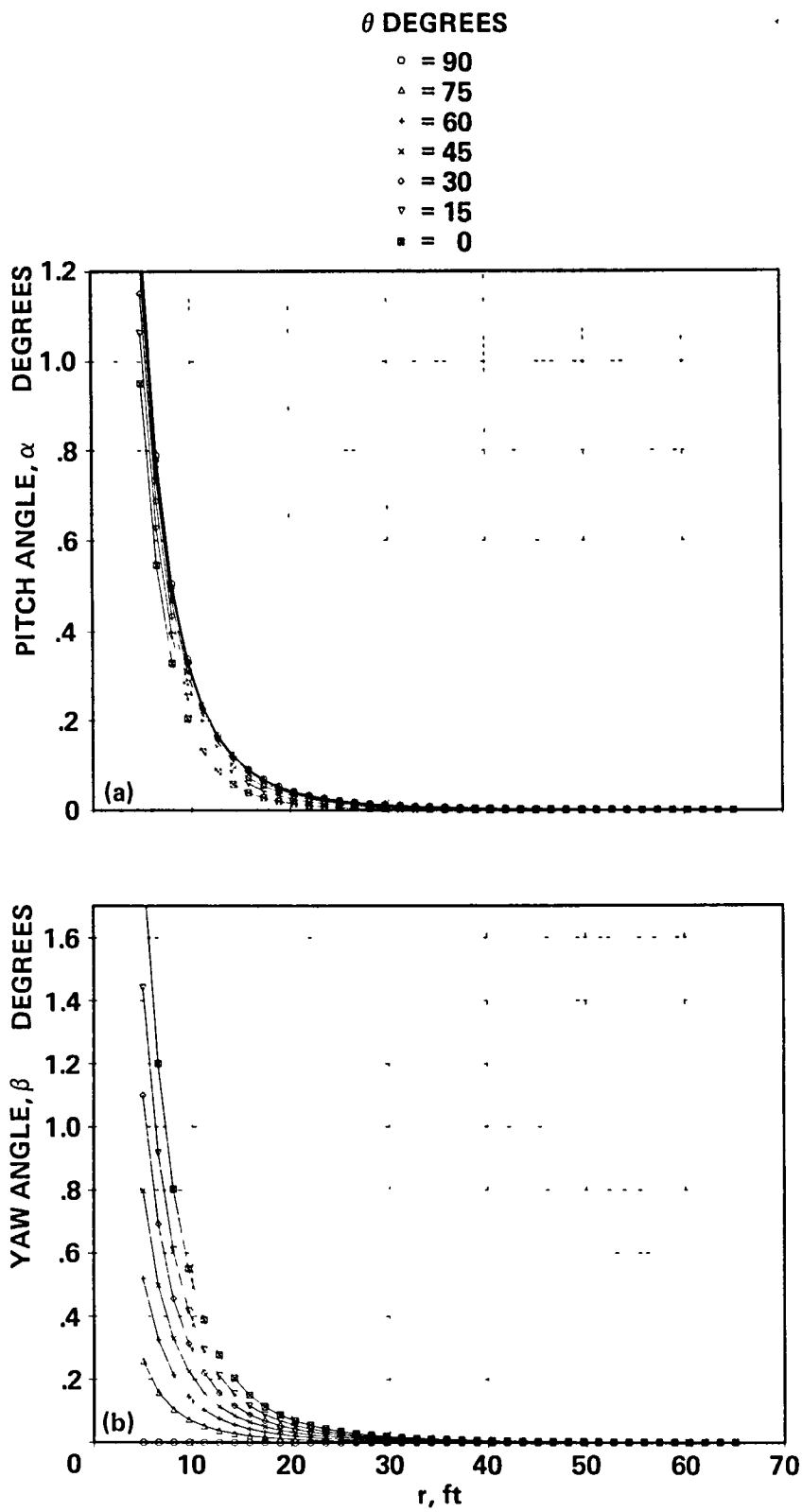

Figure 8.- Predicted values of flow angularity present in the Measurement Plane of the free-air case (a) pitch angle, (b) yaw angle.

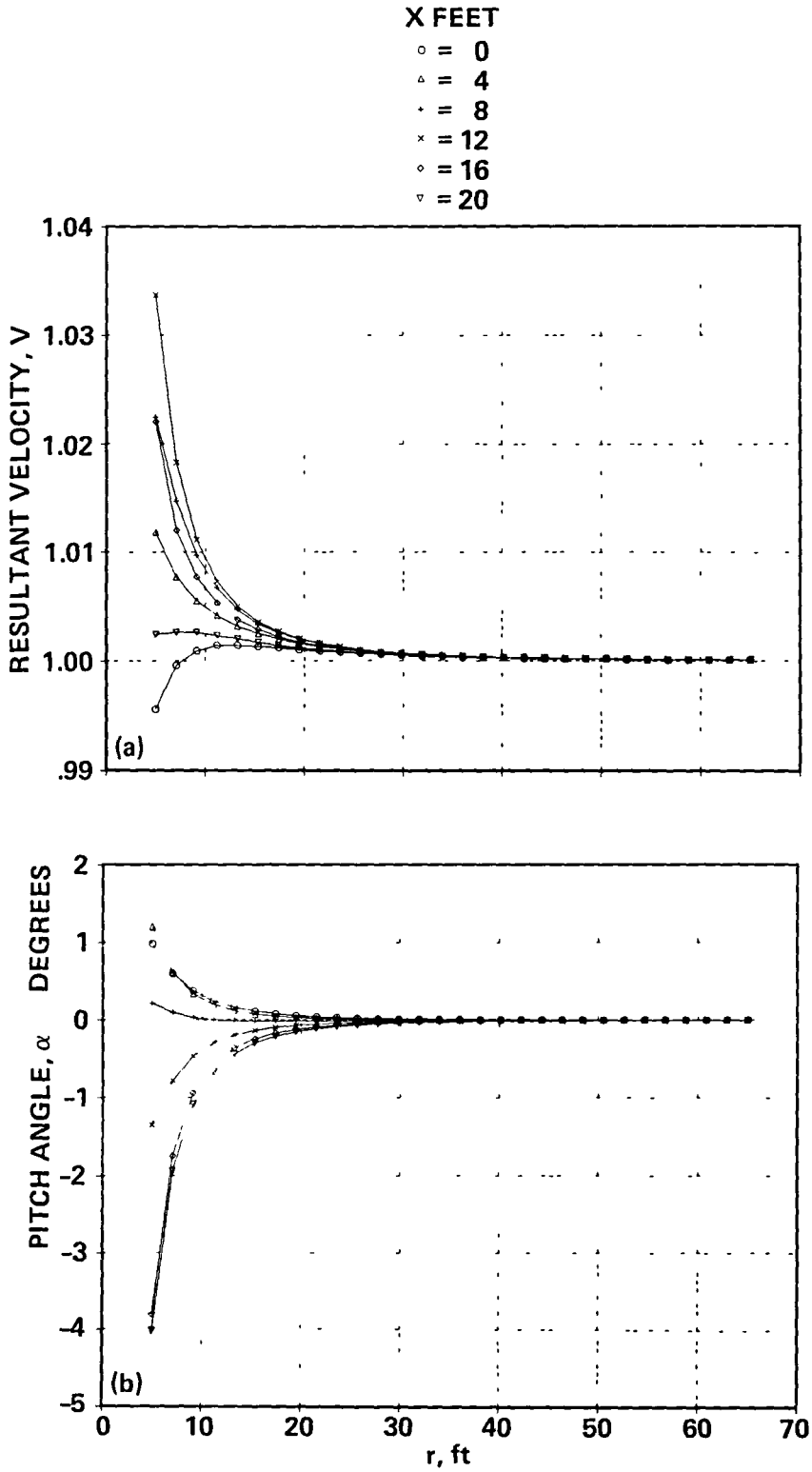

Figure 9.- Flow-field predictions versus radial distance, r, at $\theta = 90°$ for each transverse plane of the free-air case (a) resultant velocity, (b) pitch angle (yaw angularity = 0 for $\theta = 90°$ and is, therefore, not shown).

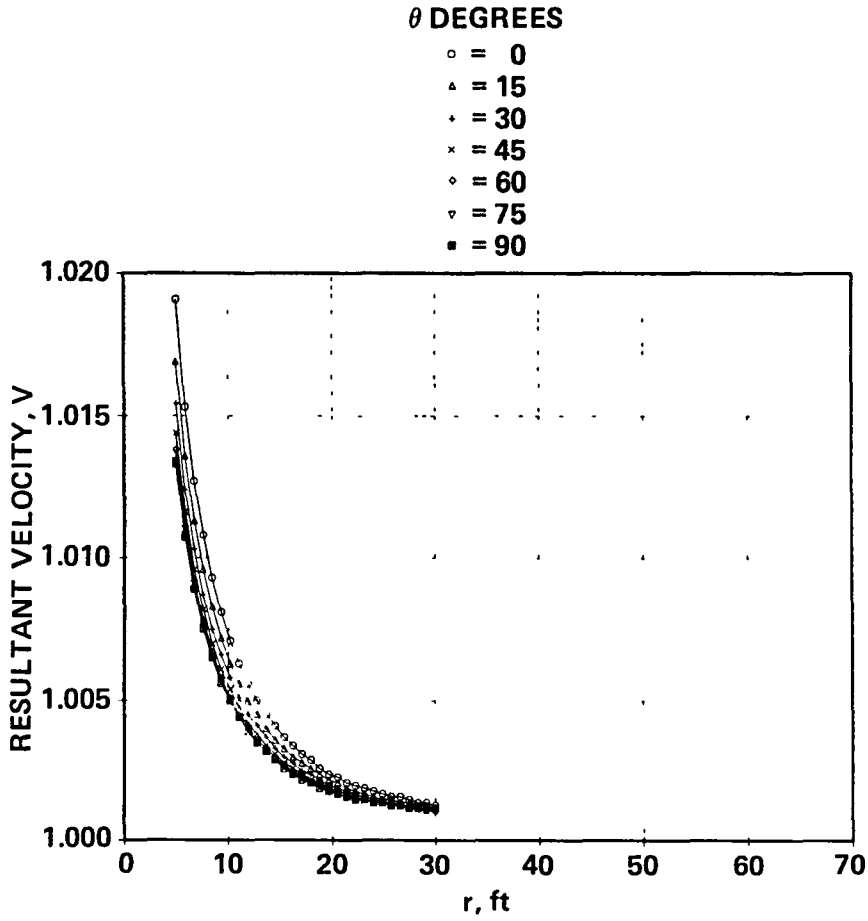

Figure 10.- Panel-code prediction of the normalized resultant velocity magnitude present in the Measurement Plane of the 40-by-80 case.

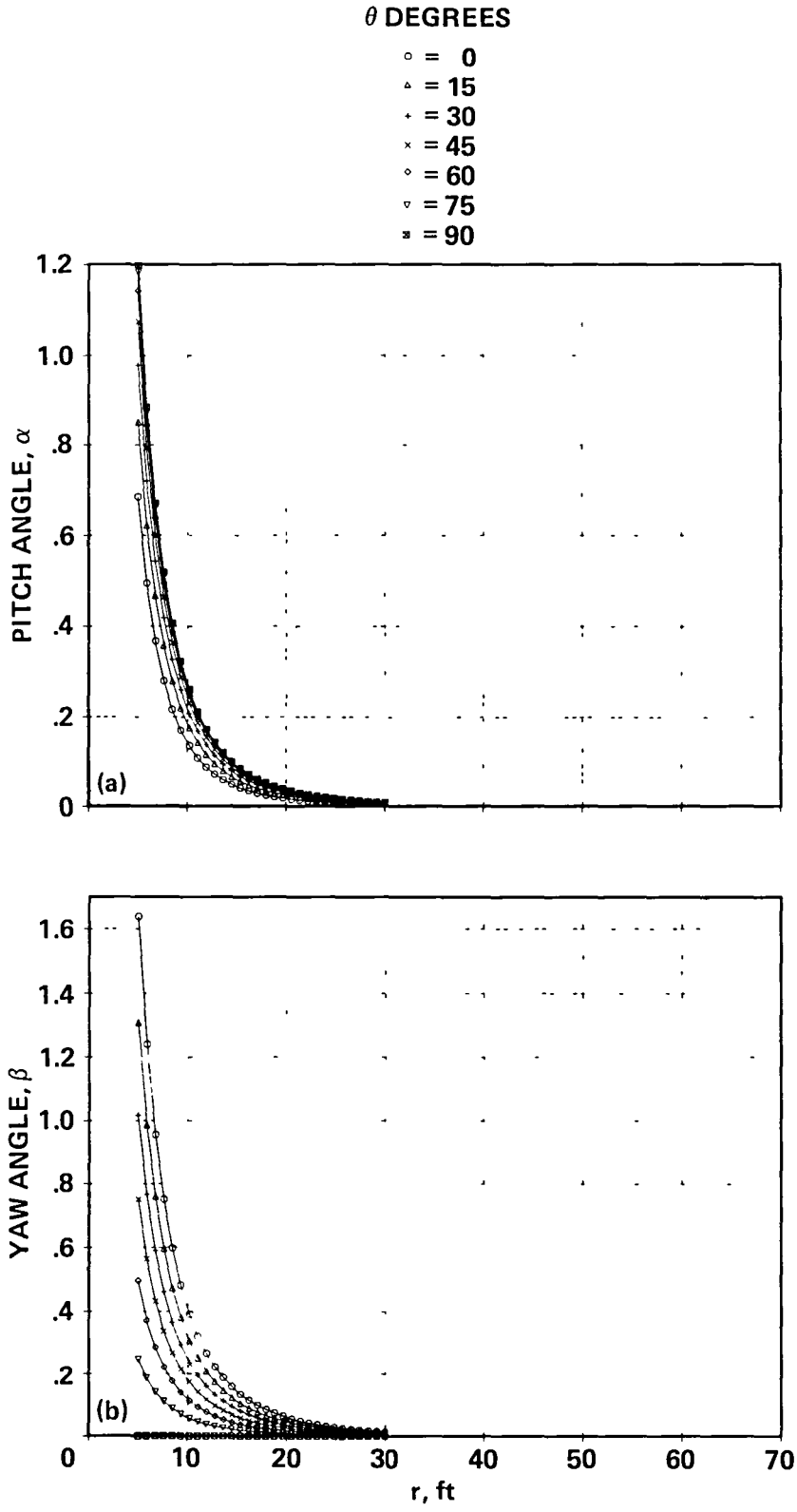

Figure 11.- Predicted values of flow angularity present in the Measurement Plane of the 40-by-80 case (a) pitch angle, (b) yaw angle.

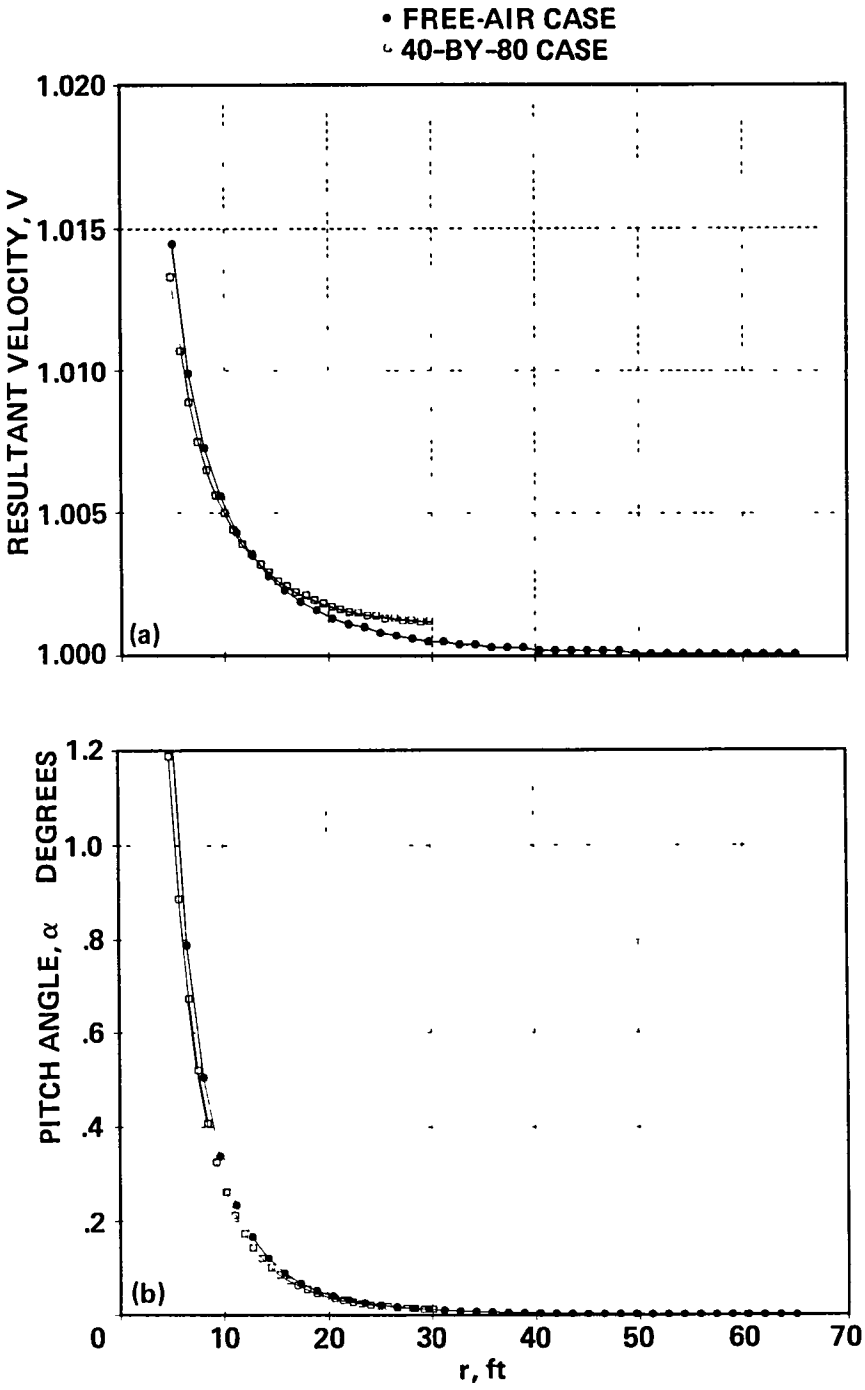

Figure 12.- Comparison of velocity and pitch angle in the Measurement Plane of the free-air and 40-by-80 cases for $\theta = 90°$.

1 Report No	2 Government Accession No.	3 Recipient's Catalog No
NASA TM-86763		

4 Title and Subtitle	5 Report Date
PREDICTION OF THE FLOW-FIELD INTERFERENCE INDUCED BY THE LONG-RANGE LASER VELOCIMETER IN THE AMES 40- BY 80-FOOT AND 80- BY 120-FOOT WIND TUNNELS	August 1985
	6 Performing Organization Code

7 Author(s)	8 Performing Organization Report No
Michael S. Reinath and James C. Ross	85286
	10 Work Unit No
	505-31-51

9 Performing Organization Name and Address	11 Contract or Grant No
Ames Research Center Moffett Field, CA 94035	
	13 Type of Report and Period Covered
12 Sponsoring Agency Name and Address	Technical Memorandum
National Aeronautics and Space Administration Washington, DC 20546	14 Sponsoring Agency Code

15 Supplementary Notes

Point of contact: Michael S. Reinath, Ames Research Center, MS 247-1, Moffett Field, CA 94035
(415)694-6680 or FTS 464-6680

16 Abstract

The predicted flow disturbances induced in the test sections of the Ames 40- by 80-Foot Wind Tunnels by the presence of the Long-Range Laser Velocimeter (LRLV) are presented. The predictions were made using a potential-flow paneling code to model the test section and the LRLV, and a calculation of the resulting flow field was made. The flow velocity and angularity were calculated at numerous locations in the flow field relative to the LRLV, and the results are presented.

17 Key Words (Suggested by Author(s))	18 Distribution Statement
Laser Doppler velocimeter Wind-tunnel interference Panel method Internal flow Long range	Unlimited Subject Category - 09

19 Security Classif (of this report)	20 Security Classif (of this page)	21 No of Pages	22 Price*
Unclassified	Unclassified	20	A02

*For sale by the National Technical Information Service, Springfield, Virginia 22161

End of Document